Original Article

Comparison of the monoexponential and biexponential models of diffusion-weighted magnetic imaging in grading clear-cell renal cell carcinoma: a case-control study

Jinfeng Cao[1]^, Jinye Dong[2], Ge Su[3], Baohua Zhang[4], Lingchen Zhu[1], Min Wang[1], Qilin Li[1], Lesong Zhang[1], Dejian Wang[5], Xin Luo[1]^

[1]Department of Radiology, Zibo Central Hospital, Zibo, China; [2]Department of Ultrasound, Weifang People's Hospital, Weifang, China; [3]College of Computer Science and Technology, Zhejiang University, Hangzhou, China; [4]Department of Pathology, Zibo Central Hospital, Zibo, China; [5]Department of R&D, Hangzhou Healink Technology, Hangzhou, China

Contributions: (I) Conception and design: J Cao, X Luo; (II) Administrative support: J Cao, J Dong, X Luo; (III) Provision of study materials or patients: J Cao, B Zhang, L Zhang; (IV) Collection and assembly of data: J Cao, M Wang, Q Li; (V) Data analysis and interpretation: J Cao, G Su; (VI) Manuscript writing: All authors; (VII) Final approval of manuscript: All authors.

Correspondence to: Xin Luo, MD. Department of Radiology, Zibo Central Hospital, 54, Gongqingtuan West Road, Zibo 255020, China. Email: asd0601@126.com.

Background: An accurate and noninvasive method to determine the preoperative clear-cell renal cell carcinoma (ccRCC) pathological grade is of great significance for surgical program selection and prognosis assessment. Previous studies have shown that diffusion-weighted imaging (DWI) has moderate value in grading ccRCC. But DWI cannot reflect the diffusion of tissue accurately because it is calculated using a monoexponential model. Intravoxel incoherent motion (IVIM) is the biexponential model of DWI. Only a few studies have examined the value of IVIM in grading ccRCC yet with inconsistent results. This study aimed to compare the value of DWI and IVIM in grading ccRCC.

Methods: In this study, 96 patients with pathologically confirmed ccRCC were evaluated by DWI and IVIM on a 3-T scanner. According to the World Health Organization/International Society of Urological Pathology (WHO/ISUP) classification system, these patients were divided into two groups: low-grade (grade I and II) and high-grade (grade III and IV) ccRCC. The apparent diffusion coefficient (ADC), true diffusion coefficient (D), pseudodiffusion coefficient (D*), and perfusion fraction of pseudodiffusion (*f*) values were calculated. The Mann-Whitney test, receiver-operating characteristic (ROC) analysis, and the Delong test were used for statistical evaluations.

Results: (I) According to the WHO/ISUP nuclear grading system, 96 patients were divided into low-grade (grade I and II, 45 patients) and high-grade (grade III and IV, 51 patients) groups. (II) Compared with patients of low-grade ccRCC, the ADC and D values of those with high-grade ccRCC decreased while the D* and *f* values increased (P<0.05). (III) The cutoff value of the ADC, D, D*, and *f* in distinguishing low-grade from high-grade ccRCC was 1.50×10^{-3} mm^2/s, 1.12×10^{-3} mm^2/s, and 33.19×10^{-3} mm^2/s, 0.31, respectively; the area under the curve (AUC) for the ADC, D, D*, and *f* values was 0.871, 0.942, 0.621, and 0.894, respectively, with the AUC of the D value being the highest; the sensitivity for the ADC, D, D*, and *f* values was 94.12%, 92.16%, 47.06%, and 92.16%, respectively; and the specificity for the ADC, D, D*, and *f* values was 66.67%, 91.11%, 77.78%, and 73.33%, respectively. (IV) Based on the Delong test, AUC_D was significantly higher than AUC_{ADC} (P=0.02) and AUC_{D^*} (P<0.001), but there was no significant difference between AUC_D and AUC_f (P=0.18).

Conclusions: Compared with the monoexponential model DWI, the biexponential model IVIM was more accurate in grading ccRCC.

^ ORCID: Jinfeng Cao, 0000-0002-5388-0991; Xin Luo, 0000-0003-4346-3956.

Keywords: Clear-cell renal cell carcinoma (ccRCC); diffusion-weighted imaging (DWI); intravoxel incoherent motion (IVIM); World Health Organization/International Society of Urological Pathology nuclear grading system (WHO/ISUP nuclear grading system)

Submitted Mar 24, 2024. Accepted for publication May 20, 2024. Published online May 28, 2024.
doi: 10.21037/tau-24-141
View this article at: https://dx.doi.org/10.21037/tau-24-141

Introduction

Clear-cell renal cell carcinoma (ccRCC) has a high incidence, strong invasiveness, and high mortality (1). In the World Health Organization/International Society of Urological Pathology (WHO/ISUP) nuclear grading system, ccRCC is classified into grades I to IV according to the degree of nucleolus saliency of tumor cells (2). Different grades of ccRCC have different degrees of malignancy and prognoses. For low-grade ccRCC, laparoscopic or local nephrectomy and other less traumatic surgery can be used; moreover, compared with the low-grade ccRCC, high-grade ccRCC is more likely to be associated with postoperative recurrence and have a higher tumor-related mortality (3). Therefore, accurate prediction of preoperative pathological grade is of great significance for surgical program selection and prognosis assessment. At present, biopsy is the gold standard to determine the pathological grading of ccRCC before surgery. However, biopsy is invasive, and involves the risks of puncture failure, postoperative bleeding, and infection, while also showing low reliability for heterogeneous tumor grading, which may differ from surgical pathological results (4). Therefore, a new accurate and noninvasive method is needed to determine the pathological grading of ccRCC.

Functional magnetic resonance imaging (fMRI) can evaluate and predict the occurrence, development, and prognosis of diseases from both morphological and functional changes, which expands the research scope of imaging diagnosis, opens numerous opportunities for clinical application research, and has great potential in grading ccRCC before surgery.

A previous study has shown that diffusion-weighted imaging (DWI) has moderate value in predicting the pathological grading of ccRCC (5). However, the apparent diffusion coefficient (ADC) value is calculated using the monoexponential model of DWI, which includes not only the diffusion (movement of water molecules) but also the perfusion effects (microcirculation of blood in capillaries); therefore, the ADC value cannot reflect the diffusion of tissue accurately. Intravoxel incoherent motion (IVIM) is a new fMRI technology developed on the basis of DWI, which can noninvasively display the subtle structural changes of tissues. IVIM is the biexponential model of DWI. It has been successfully applied in the research of central nervous system, breast lesions, prostate tumors, and other diseases (6-9). However, only a few studies have examined the value of IVIM in grading ccRCC, with inconsistent results (10-12). Zhu *et al.* (10) found that the differences between D* and *f* value of the high- and low-grade ccRCC were statistically significant (P<0.05), but Ye *et al.* (11) showed that these differences were not significant (P>0.05).

The purpose of this study was thus to compare the value of IVIM-derived parameters and ADC value in

Highlight box

Key findings

- The biexponential model intravoxel incoherent motion (IVIM) was more effective in grading clear-cell renal cell carcinoma (ccRCC) than the monoexponential model of diffusion-weighted imaging (DWI).

What is known and what is new?

- DWI has been proved to be useful in grading of ccRCC, but it cannot reflect the diffusion of tissue accurately. Only a few studies have examined the value of IVIM in grading ccRCC, with inconsistent results.
- Compared with the low-grade ccRCC group, the apparent diffusion coefficient (ADC) and true diffusion coefficient (D) values were significantly decreased in the high-grade ccRCC group while the pseudodiffusion coefficient (D*) and perfusion fraction of pseudodiffusion (*f*) values were significantly increased. The area under the curve of D value was higher than that of ADC, D*, and *f* values.

What is the implication, and what should change now?

- The results of this study showed that IVIM in the biexponential model was more valuable in grading ccRCC than DWI in the monoexponential model. Further studies with a larger sample size should be performed to investigate the value of more different diffusion models in grading ccRCC.

grading ccRCC. We present this article in accordance with the STARD reporting checklist (available at https://tau.amegroups.com/article/view/10.21037/tau-24-141/rc).

Methods

The study was conducted in accordance with the Declaration of Helsinki (as revised in 2013). Written informed consent was obtained from each patient. The case-control study was approved by institutional ethics committee of Zibo Central Hospital (No. 201907026).

Patients

From August 2019 to June 2022, 142 patients with undetermined renal masses in Zibo Central Hospital were prospectively included for magnetic resonance imaging (MRI) examinations (including DWI and IVIM). The exclusion criteria were as follows: (I) malignancy other than ccRCC as indicated by histopathological results (n=26), (II) MRI images with poor quality or obvious artifacts (n=8), (III) incomplete MRI data for DWI and IVIM (n=7), and (IV) difficulty in identifying solid components of ccRCC lesions (n=5). The cases with pathological results that were not ccRCC included the following: papillary RCC (n=9), chromophobe RCC (n=6), RCC with sarcomatous transformation (n=3), fat-poor angiomyolipoma (n=5), and renal oncocytoma (n=3).

MRI examination

MRI examinations were performed on all patients using a 3.0 T scanner (Signa Excite HD; GE HealthCare, Milwaukee, USA) and a 16-channel body phase array coil. A routine multiparametric magnetic resonance (MR) protocol was used and the procedure included transverse T2-weighted imaging with fat suppression, T1-weighted in-and-out-of-phase imaging, and multiphase dynamic contrast-enhanced (DCE) T1-weighted imaging. DWI and IVIM were acquired in the transverse plane via respiratory triggered spin echo-echo planar imaging (EPI). The sequence parameters for DWI were as follows: single-shot echo-planar imaging sequence with parallel imaging technique, transverse free breathing, b value =800 s/mm^2, time to repetition (TR)/time to echo (TE) =5,400/64 ms, field of view (FOV) =410 mm, section thickness =5.0 mm, layer spacing =1.0 mm, number of slices =19, image matrix =128×128, and scan time =1 min. Meanwhile, the parameters for IVIM were as follows: a transverse free-breathing twice-refocused spin echo, bipolar gradient, single-shot echo planar sequence, with TR/TE =5,500/60 ms, FOV =410 mm, section thickness =5.0 mm, layer spacing =1.0 mm, number of slices =19, matrix =128×128, 11 b values (0, 20, 30, 50, 100, 150, 200, 400, 600, 800, 1,000 s/mm^2), and scan time =5 min 41 s. The scanning center level of DWI was consistent with that of IVIM.

Imaging analysis

The Functool software package in the Advantage Workstation 4.5 (GE HealthCare) was used for DWI and IVIM image postprocessing and analysis. The ADC maps of DWI, true diffusion coefficient (D), pseudodiffusion coefficient (D*), and perfusion fraction of pseudodiffusion (*f*) maps of IVIM were calculated.

The DWI and IVIM images were processed by two radiologists with 7 years (L.Z.) and 15 years (M.W.) of experience in MRI diagnosis, respectively, who were unaware to the pathological grades. Based on T2-weighted imaging and DCE-MRI images, the solid areas were determined. The solid areas with the most obvious enhancement of tumors were selected as the regions of interest (ROIs) for DWI and IVIM, with cystic lesions, bleeding, and necrotic areas being avoided. Free-hand ROIs were outlined around the tumor on ADC maps and were copied to the D, D*, and *f* maps, respectively, and the corresponding parameter values were automatically generated.

Histopathological examination

After radical or partial nephrectomy, hematoxylin and eosin (HE) staining was performed on the histological sections. Based on the WHO-ISUP nuclear grading system, pathological grades I–IV were assigned for each case by a uropathologist (B.Z.) with 16 years of experience in uropathology who did not know the patient's MRI findings (2). The grading followed the highest principle; that is, when there was heterogeneity in the tissue of tumor, the highest grading was considered as the final grading.

Statistical analysis

The sample size was calculated using PASS software (Power Analysis and Sample size, v. 15.0.5). The calculation was done based on two-tailed test, α of 0.05, and power of 0.8, the

Table 1 Parameters of DWI and IVIM in low-grade and high-grade ccRCC

DWI/IVIM parameters	Low-grade ccRCC, mean ± standard deviation	High-grade ccRCC, mean ± standard deviation	W value	P value
ADC value ($\times10^{-3}$ mm^2/s)	1.63±0.16	1.36±0.19	1,999	<0.001
D value ($\times10^{-3}$ mm^2/s)	1.43±0.19	0.99±0.18	2,161.5	<0.001
D* value ($\times10^{-3}$ mm^2/s)	32.53±1.96	33.36±2.26	870	0.042
f value	0.29±0.03	0.34±0.02	243	<0.001

DWI, diffusion-weighted imaging; IVIM, intravoxel incoherent motion; ccRCC, clear-cell renal cell carcinoma; ADC, apparent diffusion coefficient; D, true diffusion coefficient; D*, pseudodiffusion coefficient; *f*, perfusion fraction of pseudodiffusion.

ratio of sample size between low-grade and high-grade group was 1:1. From previous study (10), the D value was used as the main observation indicator. The data of our preliminary experiment were used for sample size calculation.

Interobserver agreement of parameter measurements was assessed by using the intraclass correlation coefficient (ICC) with 95% confidence interval (CI). An ICC greater than 0.75 represented good agreement.

The ADC, D, D*, and *f* values between the low-grade (grade I and II) and high-grade (grade III and IV) groups were compared using the Mann-Whitney test. Receiver-operating characteristic (ROC) analysis was performed to evaluate the diagnostic performance of the DWI and IVIM parameters in grading ccRCC. Sensitivity and specificity were calculated at cut-off values providing the highest sensitivity. The Delong test was used to compare the ROCs of every two grades.

All statistical analyses were performed using SPSS (v. 21.0; IBM Corp.). Differences with P values <0.05 were considered significant (two-sided).

Results

The estimated sample size was 62 participants. While the total sample size in our study was 96 participants. Therefore, the total sample size for this study is sufficient to meet the accuracy requirements of the study.

A total of 96 patients with ccRCC were included (52 men and 44 women; age range 29–81 years; mean age 57.5 years) in the final cohort. According to the WHO/ISUP nuclear grading system, all patients were divided into low-grade (grade I and II) and high-grade (grade III and IV) groups. Of the 96 patients with ccRCC in this study, 12 were grade I, 33 were grade II, 28 were grade III, and 23 were grade IV.

The agreements between two observers for DWI and IVIM parameters were perfect. The ICC (95% CI) of the ADC, D, D*, and *f* values was 0.968 (95% CI: 0.965–0.973), 0.990 (95% CI: 0.986–0.994), 0.914 (95% CI: 0.897–0.920), and 0.935 (95% CI: 0.923–0.943), respectively.

The ADC, D, D*, and *f* values for the low-grade and high-grade ccRCC groups were (1.63±0.16)$\times10^{-3}$ mm^2/s and (1.36±0.19)$\times10^{-3}$ mm^2/s, (1.43±0.19)$\times10^{-3}$ mm^2/s and (0.99±0.18)$\times10^{-3}$ mm^2/s, (32.53±1.96)$\times10^{-3}$ mm^2/s and (33.36±2.26)$\times10^{-3}$ mm^2/s, and 0.29±0.03 and 0.34±0.02, respectively. Compared with the low-grade ccRCC group, the ADC and D values were significantly decreased in the high-grade ccRCC group while the D* and *f* values were significantly increased (P<0.05) (*Table 1*, *Figure 1*). The images of patients from the low-grade and high-grade ccRCC groups are shown in *Figures 2*,*3*.

The ROC analysis [area under the curve (AUC), sensitivity, specificity, accuracy, and cutoff value] for the ADC, D, D*, and *f* values for differentiating low-grade and high-grade ccRCC is presented in *Table 2*. The cutoff value of the ADC, D, D*, and *f* values was 1.50$\times10^{-3}$ mm^2/s, 1.12$\times10^{-3}$ mm^2/s, and 33.19$\times10^{-3}$ mm^2/s, and 0.31, respectively. Meanwhile, the AUC value for the ADC, D, D*, and *f* values was 0.871, 0.942, 0.621, and 0.894, respectively, among which the AUC of the D value was the highest (*Figure 4*).

According to the Delong test, AUC_D was significantly higher than AUC_{ADC} (P=0.02) and AUC_{D^*} (P<0.001), and there was no significant difference between AUC_D and AUC_f (P=0.18) (*Table 3*).

Discussion

This study compared the monoexponential model DWI with the biexponential model IVIM in their ability to predict the pathological grading of ccRCC. The results showed that with the increase of pathological grade of ccRCC, the ADC and D values significantly decreased the

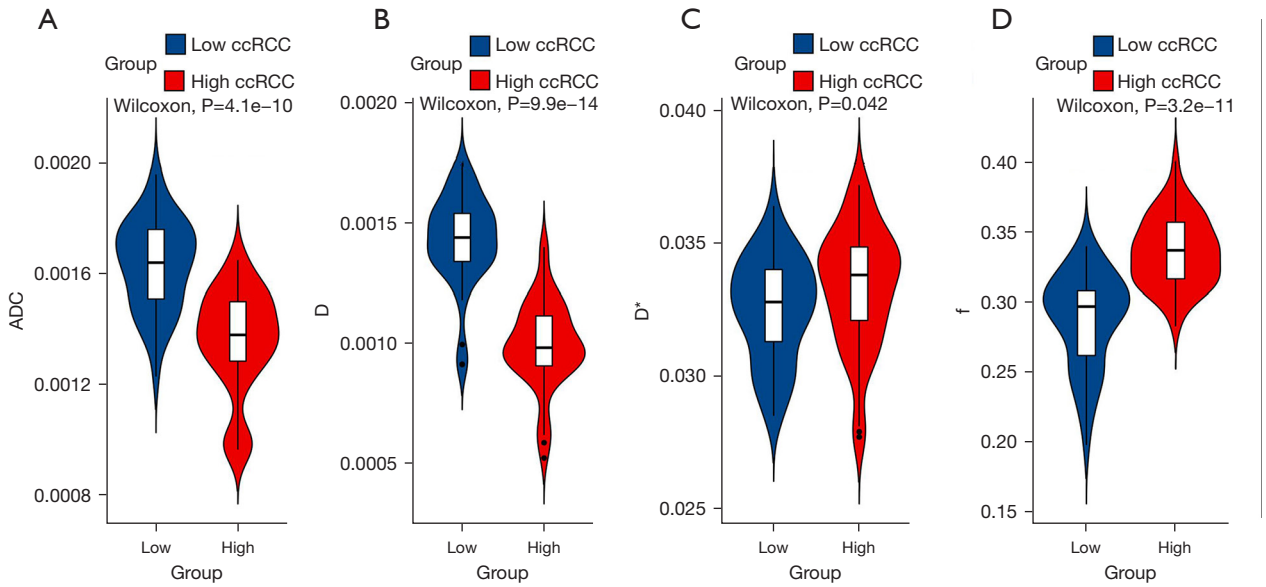

Figure 1 Comparison of parameters of DWI and IVIM in low-grade and high-grade ccRCC. ccRCC, clear-cell renal cell carcinoma; ADC, apparent diffusion coefficient; D, true diffusion coefficient; D*, pseudodiffusion coefficient; *f*, perfusion fraction of pseudodiffusion; DWI, diffusion-weighted imaging; IVIM, intravoxel incoherent motion.

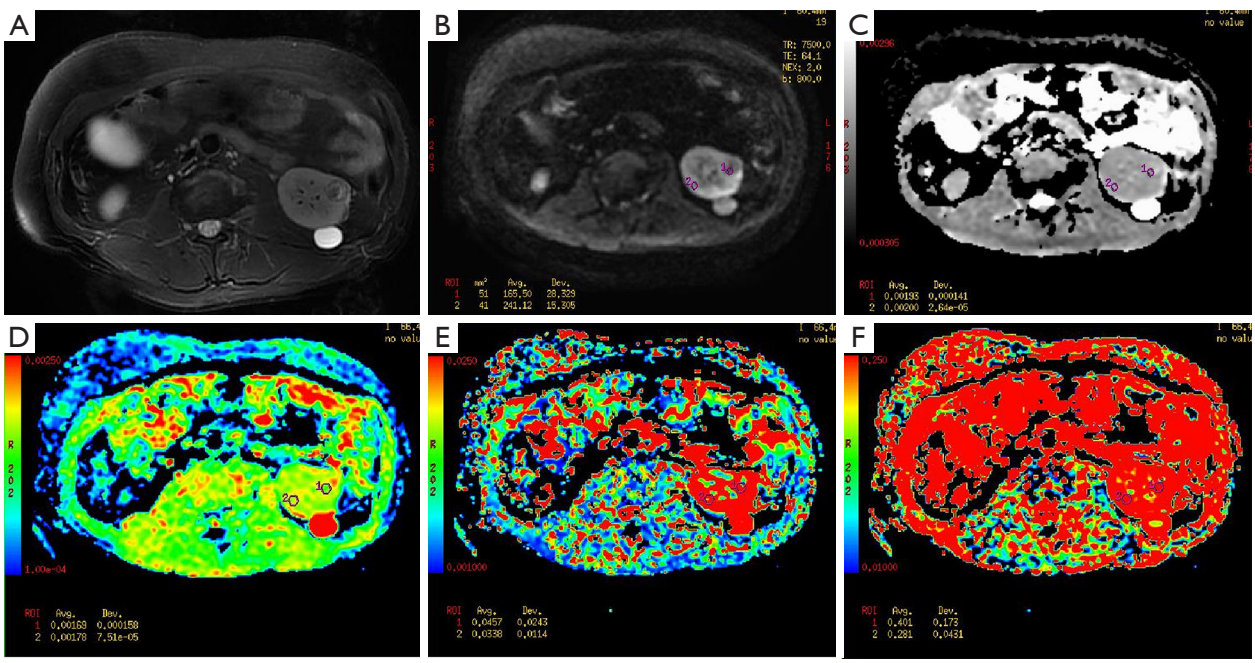

Figure 2 A 65-year-old male with a left renal tumor was surgically and pathologically confirmed to have grade II ccRCC. (A) FS-T2WI image. (B) DWI image. (C) ADC image. (D) IVIM-D image. (E) IVIM-D* image. (F) IVIM-*f* image. TR, time to repetition; TE, time to echo; ROI, region of interest; ccRCC, clear-cell renal cell carcinoma; FS-T2WI, T2-weighted imaging with fat suppression; DWI, diffusion-weighted imaging; ADC, apparent diffusion coefficient; IVIM, intravoxel incoherent motion; D, true diffusion coefficient; D*, pseudodiffusion coefficient; *f*, perfusion fraction of pseudodiffusion.

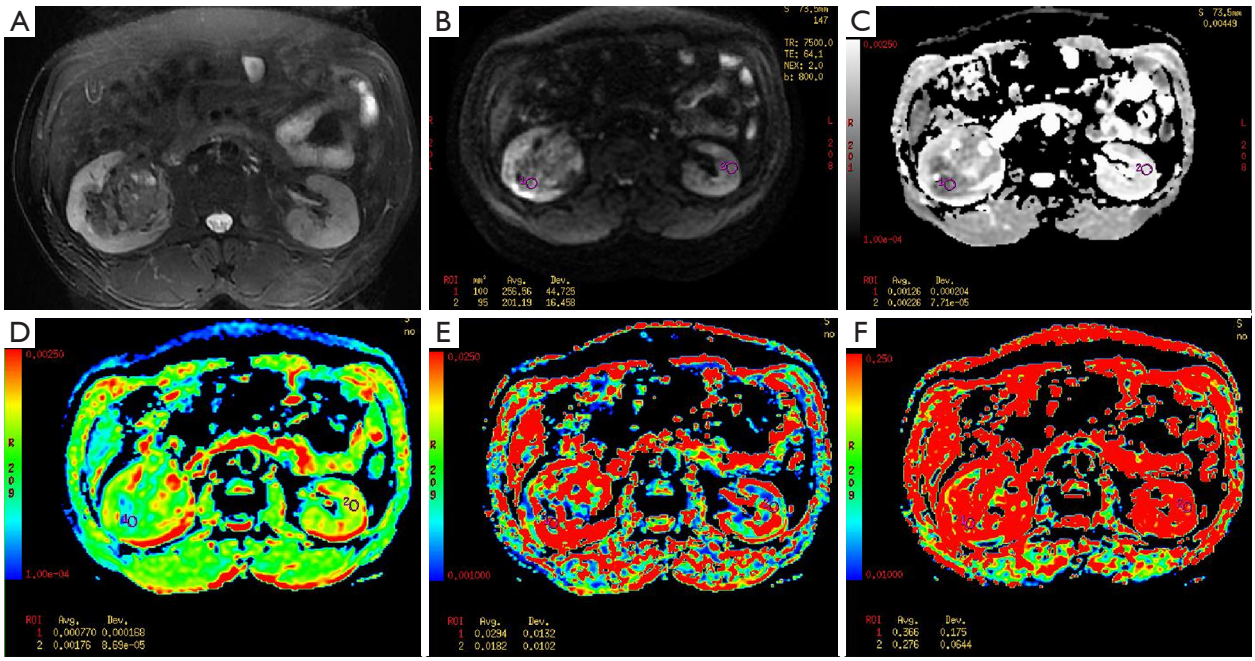

Figure 3 A 52-year-old male patient with a right renal tumor was surgically and pathologically confirmed to have grade III ccRCC. (A) FS-T2WI image. (B) DWI image. (C) ADC image. (D) IVIM-D image. (E) IVIM-D* image. (F) IVIM-*f* image. TR, time to repetition; TE, time to echo; ROI, region of interest; ccRCC, clear-cell renal cell carcinoma; FS-T2WI, T2-weighted imaging with fat suppression; DWI, diffusion-weighted imaging; ADC, apparent diffusion coefficient; IVIM, intravoxel incoherent motion; D, true diffusion coefficient; D*, pseudodiffusion coefficient; *f*, perfusion fraction of pseudodiffusion.

Table 2 ROC analysis of DWI and IVIM parameters to distinguish low-grade and high-grade ccRCC

DWI/IVIM parameters	AUC (95% CI)	Sensitivity (%)	Specificity (%)	Accuracy (%)	Cutoff value
ADC	0.871 (0.801–0.941)	94.12	66.67	81.25	1.50×10^{-3} mm^2/s
D	0.942 (0.890–0.993)	92.16	91.11	91.67	1.12×10^{-3} mm^2/s
D*	0.621 (0.508–0.733)	47.06	77.78	61.46	33.19×10^{-3} mm^2/s
f	0.894 (0.833–0.955)	92.16	73.33	83.33	0.31

ROC, receiver-operating characteristic; DWI, diffusion-weighted imaging; IVIM, intravoxel incoherent motion; ccRCC, clear-cell renal cell carcinoma; AUC, area under the curve; CI, confidence interval; ADC, apparent diffusion coefficient; D, true diffusion coefficient; D*, pseudodiffusion coefficient; *f*, perfusion fraction of pseudodiffusion.

while D* and *f* values significantly increased (P<0.05). ROC analysis showed the AUC of the D value was higher than that of the ADC, D*, and *f* values, and the results showed that IVIM in the biexponential model was more valuable in grading ccRCC than DWI in the monoexponential model, which is consistent with other study (12).

The traditional monoexponential model DWI can reflect the diffusion of water molecules and indirectly reflect the characteristics of the microstructure of tissues. DWI has been widely used in the evaluation of the pathological grade of glioma, breast cancer, rectal cancer, and other tumors (13-15). The results of this study showed that the ADC value of high-grade ccRCC was lower than that of low-grade ccRCC (P<0.05), which is consistent with the results of previous studies (16,17). These findings may be attributable to the tumor cell density of ccRCC. Compared with low-grade ccRCC, high-grade ccRCC tumor cells have more obvious atypia, larger nucleoli, smaller extracellular space, and more significant limited water molecular diffusion movement, so the ADC value is lower. However, the ADC

value obtained by the monoexponential model DWI cannot accurately reflect the degree of water molecular diffusion because of the influence of microcirculation.

IVIM was first proposed by Le Bihan *et al.* (18). As an advanced fMRI technique, IVIM can calculate both the true molecular diffusion of tissue and the microcapillary perfusion of tissues via the biexponential model. The parameters of IVIM include D, D*, and *f* values. The D value represents the pure molecular diffusion of tissues, D* value represents the pseudodiffusion coefficient, and *f* value represents the perfusion fraction of the diffusion linked to microcirculation.

Some previous studies have demonstrated that IVIM can be used to evaluate the preoperative pathological grading of glioma (19), breast cancer (20), prostate cancer (8), and other tumors, which might provide more accurate information about water diffusion. However, little research has been conducted on the application of IVIM in renal tumors, of which the focus is typically on the differentiation of benign and malignant kidney tumors or the differential diagnosis of different subtypes of renal cell carcinoma. Meanwhile, only a few preliminary studies have been conducted on the value of IVIM for the preoperative pathological grading of ccRCC (10,11).

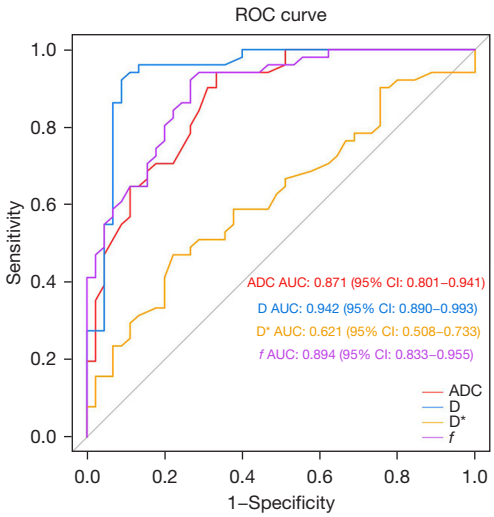

Figure 4 ROC curve of the DWI and IVIM parameters for predicting the pathological grade of ccRCC. ROC, receiver-operating characteristic; ADC, apparent diffusion coefficient; AUC, area under the curve; CI, confidence interval; D, true diffusion coefficient; D*, pseudodiffusion coefficient; *f*, perfusion fraction of pseudodiffusion; DWI, diffusion-weighted imaging; IVIM, intravoxel incoherent motion; ccRCC, clear-cell renal cell carcinoma.

The results of this study showed that compared with low-grade ccRCC, high-grade ccRCC had a lower D value but higher D* and *f* values (P<0.05), indicating that IVIM could predict the preoperative pathological grading of ccRCC. The D value reflects the true diffusion of water molecules in the tumor. In this study, the AUC (0.942) of the D value was higher than that of the ADC value (0.871), D* value (0.621), and *f* value (0.894), which confirmed that the IVIM of the biexponential model was superior to the monoexponential model DWI in grading ccRCC and that the D value was the most valuable parameter. The research results of Zhu *et al.* (10) and Ye *et al.* (11) also showed that the D value was helpful in identifying the pathological grade of ccRCC, which is in line with the results of this study, further indicating that the D value has good stability.

Both the D* and *f* values belong to the perfusion parameters of IVIM, and the results concerning the utility of the D* and *f* values in predicting the pathological grading of ccRCC are controversial. Zhu *et al.* (10) found that the D* and *f* value could distinguish high- and low-grade ccRCC and that with the increase of pathological grade, the D* value decreased while the *f* value increased (P<0.05). Shi *et al.* (12) reported that the D* value of high-grade ccRCC was slightly lower than that of low-grade ccRCC (P>0.05) while the *f* value was slightly higher, but these differences were not significant (P>0.05). The study of Ye *et al.* (11) showed that compared with that of low-grade ccRCC, the D* value of high-grade ccRCC was slightly decreased while the *f* value was slightly increased, but these differences were

Table 3 Comparison of ROC analysis results of the DWI and IVIM parameters according to the Delong test

Value	AUC_{ADC}/AUC_{D}	AUC_{ADC}/AUC_{D^*}	AUC_{ADC}/AUC_{f}	AUC_{D}/AUC_{D^*}	AUC_{D}/AUC_{f}	AUC_{D^*}/AUC_{f}
Z value	−2.359	4.155	−0.552	5.816	1.353	−4.650
P value	0.02	<0.001	0.58	<0.001	0.18	<0.001

ROC, receiver-operating characteristic; DWI, diffusion-weighted imaging; IVIM, intravoxel incoherent motion; ADC, apparent diffusion coefficient; D, true diffusion coefficient; D*, pseudodiffusion coefficient; *f*, perfusion fraction of pseudodiffusion.

not significant (P>0.05). Therefore, Ye *et al.* (11) indicated that the perfusion parameters of IVIM (D* and *f* values) cannot be used to differentiate the pathological grade of ccRCC.

In our study, the D* and *f* values of high-grade ccRCC were significantly higher than those of low-grade ccRCC, and the differences were statistically significant (P>0.05). This may be related to the difference of tissue vascularity between low-grade and high-grade ccRCC. ccRCC is a type of tumor with a rich blood supply, and compared with the low-grade ccRCC, high-grade ccRCC has more vascularity in the tumor tissue. The D* and *f* values are associated with perfusion and can reflect the degree of tissue vascularity; therefore, the D* and *f* value increase with the increase of the pathological grade of ccRCC.

The reasons for the instability of the D* and *f* values in the differentiation of low- and high-grade ccRCC may be related to the following phenomena: (I) the capillary network and tubule system of the kidney are abundant, so the microcirculation perfusion of the kidney is likely to be affected by various factors and changes, such as the different sites of the tumor in the kidneys. (II) High-grade ccRCC is more likely to be associated with bleeding and necrosis, and the microcirculation perfusion of the corresponding region may be relatively low. (III) The different sequence parameters used to obtain IVIM data can reflect the stability of D* and *f* values. (IV) The different sample size and pathological distribution could have an impact on these parameters. Therefore, more research is required to determine the utility, stability, and repeatability of the D* and *f* values in grading ccRCC.

In recent years, some different diffusion models have been proposed to characterize the non-Gaussian water diffusion in the aspect of tissue complexity and vascularity, such as the diffusion kurtosis imaging (DKI) model and fractional order calculus (FROC) model (12,21). DKI can reflect the tissue complexity by using higher b values and quantify the non-Gaussian behavior of diffusion and the excess kurtosis of tissue. Cheng *et al.* (21) performed a study on 65 ccRCC patients to value of quantitative parameters derived from DKI and IVIM in differentiating histologic grades. They found that both IVIM and DKI could be used to predict the pathological grade of ccRCC, and the combined utilization of the IVIM and DKI models offered enhanced diagnostic accuracy and efficiency. The FROC model can provide a multi-faceted characterization of tissues based on not only cellularity but also structural heterogeneity. Shi *et al.* (12) demonstrated that the FROC parameters were superior to ADC and IVIM parameters in grading ccRCC. The potential advantage of more different diffusion models in grading ccRCC remains to be fully explored.

The study had some limitations that should be mentioned. First, the number of patients with ccRCC was relatively small and could only be divided into low-grade and high-grade ccRCC groups. Additional studies using larger patient cohorts will be performed to include groups corresponding to grades I–IV. Second, the ROIs were selected on the solid areas with the most obvious enhancement of ccRCC instead of the entire area of tumor. This might have led to a certain degree of selection bias because of the heterogeneity of the ccRCC. Third, other advanced DWI models such as DKI were not evaluated. Further studies with a larger sample size are needed to investigate the value of more different diffusion models in grading ccRCC.

Conclusions

Both the monoexponential DWI and the biexponential IVIM models were found to be useful in differentiating low- and high-grade ccRCC, but the IVIM of the biexponential model was superior in this regard.

Acknowledgments

Funding: This research was supported by the Zibo Key Research and Development Plan (Nos. 2020ZC010169 to J.C. and 2020ZC010263 to X.L.).

Footnote

Reporting Checklist: The authors have completed the STARD reporting checklist. Available at https://tau.amegroups.com/article/view/10.21037/tau-24-141/rc

Data Sharing Statement: Available at https://tau.amegroups.com/article/view/10.21037/tau-24-141/dss

Peer Review File: Available at https://tau.amegroups.com/article/view/10.21037/tau-24-141/prf

Conflicts of Interest: All authors have completed the ICMJE uniform disclosure form (available at https://tau.amegroups.com/article/view/10.21037/tau-24-141/coif). J.C. reports grant from the Zibo Key Research and Development Plan

(No. 2020ZC010169). X.L. reports grant from the Zibo Key Research and Development Plan (No. 2020ZC010263). D.W. is from Hangzhou Healink Technology. The other authors have no conflicts of interest to declare.

Ethical Statement: The authors are accountable for all aspects of the work in ensuring that questions related to the accuracy or integrity of any part of the work are appropriately investigated and resolved. The study was conducted in accordance with the Declaration of Helsinki (as revised in 2013). The study was approved by institutional ethics committee of Zibo Central Hospital (No. 201907026) and informed consent was taken from all the patients.

References

1. Zhang HM, Wen DG, Chen J, et al. A diagnostic test of three-dimensional magnetic resonance elastography imaging for preoperative prediction of microvascular invasion in patients with T1 stage clear cell renal carcinoma. Transl Androl Urol 2023;12:466-76.
2. Moch H, Cubilla AL, Humphrey PA, et al. The 2016 WHO Classification of Tumours of the Urinary System and Male Genital Organs-Part A: Renal, Penile, and Testicular Tumours. Eur Urol 2016;70:93-105.
3. Sim KC, Han NY, Cho Y, et al. Machine Learning-Based Magnetic Resonance Radiomics Analysis for Predicting Low- and High-Grade Clear Cell Renal Cell Carcinoma. J Comput Assist Tomogr 2023;47:873-81.
4. Brummer O, Pölönen P, Mustjoki S, et al. Computational textural mapping harmonises sampling variation and reveals multidimensional histopathological fingerprints. Br J Cancer 2023;129:683-95.
5. Cao J, Luo X, Zhou Z, et al. Comparison of diffusion-weighted imaging mono-exponential mode with diffusion kurtosis imaging for predicting pathological grades of clear cell renal cell carcinoma. Eur J Radiol 2020;130:109195.
6. Gu T, Yang T, Huang J, et al. Evaluation of gliomas peritumoral diffusion and prediction of IDH1 mutation by IVIM-DWI. Aging (Albany NY) 2021;13:9948-59.
7. Uslu H, Önal T, Tosun M, et al. Intravoxel incoherent motion magnetic resonance imaging for breast cancer: A comparison with molecular subtypes and histological grades. Magn Reson Imaging 2021;78:35-41.
8. Malagi AV, Netaji A, Kumar V, et al. IVIM-DKI for differentiation between prostate cancer and benign prostatic hyperplasia: comparison of 1.5 T vs. 3 T MRI. MAGMA 2022;35:609-20.
9. Lu T, Song B, Pu H, et al. Prognosticators of intravoxel incoherent motion (IVIM) MRI for adverse maternal and neonatal clinical outcomes in patients with placenta accreta spectrum disorders. Transl Androl Urol 2020;9:258-66.
10. Zhu Q, Ye J, Zhu W, et al. Value of intravoxel incoherent motion in assessment of pathological grade of clear cell renal cell carcinoma. Acta Radiol 2018;59:121-7.
11. Ye J, Xu Q, Wang SA, et al. Quantitative Evaluation of Intravoxel Incoherent Motion and Diffusion Kurtosis Imaging in Assessment of Pathological Grade of Clear Cell Renal Cell Carcinoma. Acad Radiol 2020;27:e176-82.
12. Shi B, Xue K, Yin Y, et al. Grading of clear cell renal cell carcinoma using diffusion MRI with a fractional order calculus model. Acta Radiol 2023;64:421-30.
13. Momeni F, Abedi-Firouzjah R, Farshidfar Z, et al. Differentiating Between Low- and High-grade Glioma Tumors Measuring Apparent Diffusion Coefficient Values in Various Regions of the Brain. Oman Med J 2021;36:e251.
14. Tuan Linh L, Minh Duc N, Minh Duc N, et al. Correlations between apparent diffusion coefficient values and histopathologic factors in breast cancer. Clin Ter 2021;172:218-24.
15. Liu J, Li Q, Tang L, et al. Correlations of Mean and Mimimum Apparent Diffusion Coefficient Values With the Clinicopathological Features in Rectal Cancer. Acad Radiol 2021;28 Suppl 1:S105-11.
16. Zhu Q, Zhu W, Wu J, et al. Comparative study of conventional diffusion-weighted imaging and introvoxel incoherent motion in assessment of pathological grade of clear cell renal cell carcinoma. Br J Radiol 2022;95:20210485.
17. Mytsyk Y, Dutka I, Yuriy B, et al. Differential diagnosis of the small renal masses: role of the apparent diffusion coefficient of the diffusion-weighted MRI. Int Urol Nephrol 2018;50:197-204.
18. Le Bihan D, Breton E, Lallemand D, et al. MR imaging of intravoxel incoherent motions: application to diffusion

and perfusion in neurologic disorders. Radiology 1986;161:401-7.
19. Wang X, Chen XZ, Shi L, et al. Glioma grading and IDH1 mutational status: assessment by intravoxel incoherent motion MRI. Clin Radiol 2019;74:651.e7-651.e14.
20. Iima M, Honda M, Sigmund EE, et al. Diffusion MRI of the breast: Current status and future directions. J Magn Reson Imaging 2020;52:70-90.
21. Cheng Q, Ren A, Xu X, et al. Application of DKI and IVIM imaging in evaluating histologic grades and clinical stages of clear cell renal cell carcinoma. Front Oncol 2023;13:1203922.

Cite this article as: Cao J, Dong J, Su G, Zhang B, Zhu L, Wang M, Li Q, Zhang L, Wang D, Luo X. Comparison of the monoexponential and biexponential models of diffusion-weighted magnetic imaging in grading clear-cell renal cell carcinoma: a case-control study. Transl Androl Urol 2024;13(5):792-801. doi: 10.21037/tau-24-141

